Aqueduct pressure gradient quantified by MRI in hydrocephalus populations.

Olivier Baledent, Pan LIU, Yann Attekeble, Jiachen Xie, Heimiri Monnier, Serge Metanbou, Kimi Owashi, Cyrille Capel

0589

Aqueduct pressure gradient quantified by MRI in hydrocephalus populations.

Olivier BALEDENT[1,2], Pan LIU[1,2], Yann ATTEKEBLE[2], Jiachen XIE[2], Heimiri MONNIER[2], Serge METANBOU[3], Kimi OWASHI[1,2], and Cyrille CAPEL[2,4]
[1]Medical Image Processing, University Hospital CHU Amiens, Amiens, France, [2]Jules Verne University CHIMERE UR 7516, Amiens, France, [3]Radiology, University Hospital CHU Amiens, Amiens, France, [4]Neurosurgery, University Hospital CHU Amiens, Amiens, France

Synopsis

Keywords: Other Neurodegeneration, Neurofluids, Cerebro Spinal Fluid

Motivation: Hydrocephalus pathophysiology is not completely known and new investigations of CSF oscillations due to cardiac pulsations, probable origin of the ventricle dilation, can be helpful.

Goal(s): To calculate non-invasively intracranial pressure difference in the aqueduct in hydrocephalus patients using MRI.

Approach: We developed a dedicated software to automatically quantify the largest ventricle surface area, the CSF flow oscillations and aqueduct morphology dimensions. Using the Poiseuille equation, we calculated the intracranial pressure difference across the aqueduct.

Results: Resistance and pressure difference in the aqueduct were significantly smaller in hydrocephalus patients than in healthy populations.

Impact: Studying aging healthy individuals, hydrocephalus patients without improvement after shunt, Alzheimer's populations may reveal new biomarkers to improve diagnosis and patient selection for shunt surgery. Such investigations will deepen our knowledge of the physiopathology of ventricle dilation and CSF clearance.

Introduction:
In some hydrocephalus and misdiagnosis Alzheimer patients, dementia can be treated by a shunt surgery derivation of the CSF (1). Hydrocephalus pathophysiology is not completely known (2,3) and new investigations of the CSF oscillations due to cardiac pulsations, probable origin of the ventricle dilation (4,5), can be helpful. Aqueduct morphology and aqueduct CSF flow oscillations ($Q_{CSF}(t)$) are easily accessible by MRI (6). Aqueduct Stroke volume of CSF ($SV_{aqueduct}$) represents the CSF volume expansion of the lateral ventricles beating during cardiac cycle (4). $Q_{CSF}(t)$ is driven by a pressure difference ($\Delta P_{aqueduct}(t)$) between the third and fourth ventricles, dominated by cardiac pulsations during free brething (7) $Q_{CSF}(t)$ is also influenced by the flow resistance of the aqueduct ($R_{aqueduct}$). $\Delta P_{aqueduct}(t)=R_{aqueduct}\cdot Q_{CSF}(t)$ (6-9). It is invasive to measure intracranial pressure and difficult to calculate $\Delta P_{aqueduct}(t)$ amplitude by using sensors (~ 0.1 mmHg; ~ 13 Pa) (7). Based on biophysical knowledge of fluids mechanics and MRI measurements some authors proposed different approach to quantify non-invasively $\Delta P_{aqueduct}(t)$ (6-9). Aim of this work was to calculate non-invasively $\Delta P_{aqueduct}(t)$ in hydrocephalus patients and healthy volunteers using MRI.

Methods:
40 patients diagnosed by the neurosurgeon with suspected Normal Pressure Hydrocephalus and 36 healthy volunteers gave their ethical consent to be included in this 3T MRI research protocol. They underwent a 3D T1 to calculate ventricle surface, balanced fast field echo to quantify Raqueduct and 2D phase-contrast with finger plethysmograph to measure $Q_{CSF}(t)$ oscillations during cardiac cycle. Fig 1. Viscosity of the CSF was supposed equivalent to water viscosity. We developed a dedicated software to automatically quantify, the largest ventricle surface (area-vent), the $Q_{CSF}(t)$ oscillations, and aqueduct morphology dimensions. The software calculated Raqueduct and $\Delta P_{aqueduct}(t)$ using the Poiseuille equation. It also calculated, Q-ampli representing the Amplitude of $Q_{CSF}(t)$ and $\Delta P_{aqueduct}$ representing the amplitude of $\Delta P_{aqueduct}$ (t). It calculated Womersley and Reynolds numbers. Fig 2. We applied this new methodology on the two populations and compared the results with Mann-Whitney evaluation. We calculated histogram distribution and correlation of the parameters.

Results:
$SV_{aqueduct}$, Q-ampli and Area-vent were logically higher in patients than in volunteers. $R_{aqueduct}$ and $\Delta P_{aqueduct}$ were significantly smaller in hydrocephalus patients than in healthy populations. In Hydrocephalus population ventricles surface (area-vent) slightly correlated with $SV_{aqueduct}$ but not in healthy population in which ventricles area was negatively correlated with $\Delta P_{aqueduct}$ and $R_{aqueduct}$.

<u>In both populations:</u>

- $\Delta P_{aqueduct}$ correlated with $R_{aqueduct}$.
- $SV_{aqueduct}$ negatively correlated with $R_{aqueduct}$.
- $SV_{aqueduct}$ did not correlated with $\Delta P_{aqueduct}$.

All the results are presented in the table of Fig 3 and in the graphs of Fig 4 and Fig 5.

Discussion:
$\Delta P_{aqueduct}$ can be easily calculated non-invasively by using simple and rapid (around 10 mn) MRI sequences. Depending on the investigator's expertise, it took between 5 and 15 minutes to post process the images using new home-made software applicable in clinical practice. 2D area of the lateral ventricle rather than the total 3D segmentation was preferred by the clinicians because it is simple, rapid, robust and significantly proportional to the ventricles volume (10-11). The results obtained align with previous invasive measurements or complex numerical fluid simulations (6-9). The younger age of our healthy population limits the interpretation of differences obtained in hydrocephalus patients. Studying aging healthy individuals, hydrocephalus patients without improvement after shunt, Alzheimer's populations will give us new potential biomarkers to improve diagnosis (1-4,11). In hydrocephalus patients $\Delta P_{aqueduct}$ paradoxically decreased, nevertheless large CSF waves caused by large aqueduct diameter continuously stress the tissues surrounding the ventricles. We hypothesize that reducing the aqueduct diameter could redirect CSF flow through the subarachnoid spaces and increase glymphatic clearance in the cortical sulci. Reynolds numbers were below 2000, indicating CSF flow was not turbulent. Womersley number expresses the ratio of oscillatory inertia force to the shear force. Values below 10 suggest a non-flat velocity profile, and the flow was nearly in phase with the pressure gradient, allowing it to be approximated by Poiseuille's law using the instantaneous pressure gradient. Nevertheless, Womersley number is also higher than 1, meaning that, even if the viscous forces dominate, inertial forces exist, leading to potential small underestimation of ΔP (6,8,9). This will be corrected in the next software version using Navier-Stokes equations.

Conclusion:
Resistance of the aqueduct can be quantified with morphological MRI. CSF flow oscillations during cardiac cycle can be quantified with 2D Phase Contrast MRI. Based on Poiseuille's law, aqueduct pressure gradient driving CSF oscillations can be calculated non-invasively. In hydrocephalus patients with dilated ventricles, CSF stroke volume is increased but paradoxically $\Delta P_{aqueduct}$ is smaller than young healthy population due to small resistance of the dilated aqueduct.

Acknowledgements

This research was supported by EquipEX FIGURES (Facing Faces Institute Guilding Research), Hanuman ANR-18-CE45-0014, ANR-23-CE18-0026 and Region Haut de France. Thanks to the staff members at the Facing Faces Institute (Amiens, France) for technical assistance. Thanks to David Chechin from Phillips industry for his scientific support.

References

1. Seng PH, Huang WT, Wang JH, Huang BR, Huang HY, Tsai ST. Cerebrospinal fluid shunt surgery reduces the risk of developing dementia and Alzheimer's disease in patients with idiopathic normal pressure hydrocephalus: a nationwide population-based propensity-weighted cohort study. Fluids Barriers CNS. 2024 Feb 14;21(1):16.
2. Levine DN, Intracranial pressure and ventricular expansion in hydrocephalus: have we been asking the wrong question? J. Neurol. Sci 269 (1–2) (2008) 1–11.
3. Mani R, Basem J, Yang L, Fiore S, Djuric P, Egnor M. Review of theories into the pathogenesis of normal pressure hydrocephalus. BMJ Neurol Open. 2024 Oct 17;6(2):e000804.
4. Holmlund P, Qvarlander S, Malm J, Eklund A, Can pulsatile CSF flow across the cerebral aqueduct cause ventriculomegaly? A prospective study of patients with communicating hydrocephalus, Fluids Barriers CNS 16 (1) (2019) 1–10.
5. Eide PK, Sæhle T, Is ventriculomegaly in idiopathic normal pressure hydrocephalus associated with a transmantle gradient in pulsatile intracranial pressure? Acta Neurochir. (Wien) 152 (6) (2010) 989–995.
6. Bardan G, Plouraboué F, Zagzoule M, Baledent O, Simple patient-based transmantle pressure and shear estimate from cine phase-contrast MRI in cerebral aqueduct, IEEE Trans. Biomed. Eng 59 (10) (2012) 2874–2883.
7. Vinje, V., Ringstad, G., Lindstrøm, E.K. et al. Respiratory influence on cerebrospinal fluid flow – a computational study based on long-term intracranial pressure measurements.Sci Rep 9, 9732 (2019).
8. Sincomb S, Moral-Pulido F, Campos O, Martínez-Bazán C, Haughton V, Sánchez AL. An in vitro experimental investigation of oscillatory flow in the cerebral aqueduct. Eur J Mech B Fluids. 2024 May-Jun;105:180-191.
9. Karki P, Cogswell PM, Murphy M, Ganji1 S, Graff-Radford J, Alder B, Jones D, Huston J III, Fluid mechanics based distinct cerebrospinal fluid dynamics signature in normal pressurehydrocephalus, in: ISMRM & ISMRT Annual Meeting & Exhibition, International Society for Magnetic Resonance in Medicine, 2023
10. Chaarani B, Capel C, Zmudka J, Daouk J, Fichten A, Gondry-Jouet C, Bouzerar R, Balédent O. Estimation of the lateral ventricles volumes from a 2D image and its relationship with cerebrospinal fluid flow. Biomed Res Int. 2013;2013:215989.
11. Li H, Liu C, Tai H, Wei Y, Shen T, Yang Q, Zheng K, Xing Y. Comparison of cerebrospinal fluid space between probable normal pressure hydrocephalus and Alzheimer's disease. Front Aging Neurosci. 2023 Aug 24;15:1241237

Figures

Figure 1: Imaging acquisition and participant information for the Healthy Control (HC) Group (blue) and iNPH Group (red). Imaging locations for the three sequences are indicated on the schematic to the left. Example images and acquisition parameters for each sequence are color-coded: axial 3D T1 in brown, real-time phase contrast (perpendicular to the aqueduct) in cyan, and sagittal balanced fast field echo (BFFE) in purple.

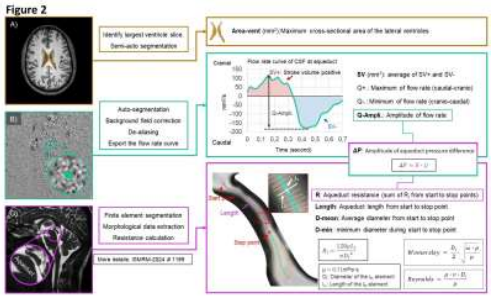

Figure 2: Image processing workflow. A) Identify the largest lateral ventricle slice and segment it to extract Area-vent. B) Segment the aqueduct in PC-MRI, apply background correction, and extract the average cardiac cycle flow curve, recording stroke volume (SV) and peak flow rate (Q-Ampli.). C) Use finite element segmentation on the aqueduct to obtain length, mean diameter (D-mean), and minimum diameter (D-min). Calculate aqueduct resistance (R) via Poiseuille's equation, with the product of R and Q-Ampli. giving the peak pressure difference (ΔP) across the aqueduct.

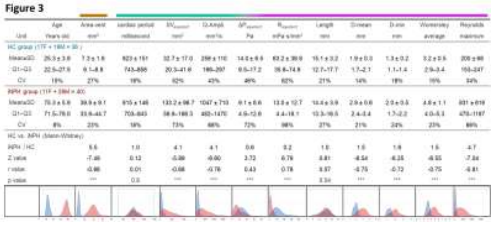

Figure 3: Table of parameters for the HC and iNPH groups, presented as mean ± SD and interquartile range (Q1–Q3). Differences between groups were assessed using Mann-Whitney test. Distribution plots of each parameter for both groups are shown at the bottom. SV: stroke volume; Q-Ampli. denotes peak flow rate; ΔP indicates peak pressure difference across the aqueduct; Womersley number between the start and end points; Maximum Reynolds number between the start and end points; CV: coefficient of variation, calculated as the standard deviation divided by the mean. D: aqueduct diameter.

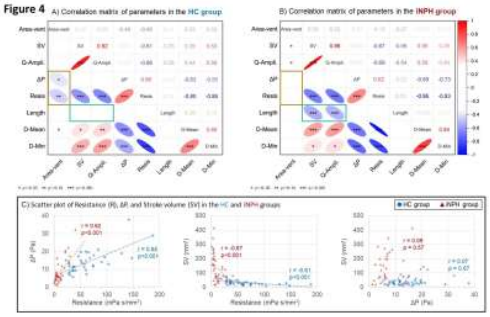

Figure 4: Correlation matrices of parameters in the HC (A) and iNPH (B) groups. SV denotes stroke volume, Resis represents aqueduct flow resistance, D-Mean is the mean aqueduct diameter, and Q-Ampli indicates peak flow rate in the aqueduct. C) Scatter plots of resistance (R), ΔP, and stroke volume (SV). Blue circles represent the HC group, and red triangles represent the iNPH group. Correlation coefficients (r) and p values are derived from Spearman's test.

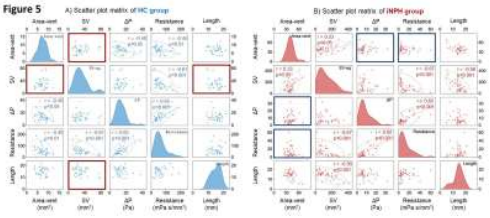

Figure 5: Scatter plot matrices for the HC (A) and iNPH (B) groups. Red boxes in (A) and blue boxes in (B) indicate pairs of parameters that lack correlation within the current group but show significant correlation in the other group. Area-vent represents the cross-sectional area of the lateral ventricles, SV denotes stroke volume of the aqueduct, ΔP indicates the peak pressure difference across the aqueduct, Resistance represents aqueduct resistance, and Length represents aqueduct length.

Proc. Intl. Soc. Mag. Reson. Med. 33 (2025)
0589

DOI: https://doi.org/10.58530/2025/0589